In-vivo usefulness of Optical Coherence Tomography in atrophic-erosive oral lichen planus: comparison between histopathological and ultrastructural findings.[1]

Alessio Gambino[1], Marco Cabras[1], Adriana Cafaro[1], Roberto Broccoletti[1], Stefano Carossa[1], Colin Hopper[2], Luigi Chiusa[3], Stephen R. Porter[2], Paolo G. Arduino[1].

[1] Department of Surgical Sciences, Oral Medicine Section, CIR-Dental School, University of Turin, Italy.

[2] Department of Clinical Research, UCL Eastman Dental Institute, London, United Kingdom.

[3] AOU Città della salute e della Scienza di Torino, Turin, Italy.

Corresponding Author:

Dr. Alessio Gambino

Department of Surgical Sciences; CIR - Dental School.

School of Medicine, University of Turin.

Oral Medicine Unit, Via Nizza 230, I-10126 Turin (Italy).

Telephone: + 390116331522; Fax: +39011618639.

E-mail: alessio.gambino@unito.it

Short Title: Use of Optical Coherence Tomography in patients with Oral Lichen Planus.

Abbreviations: OCT, optical coherence tomography; OLP, Oral Lichen Planus; EP, stratified squamous epithelium; LP, lamina propria.

---

[1]Based on a thesis submitted to the post-graduate faculty, Department of Surgical Science, University of Turin, and Politecnico of Turin, in partial fulfilment of the requirements for the PhD degree.

ABSTRACT

Oral lichen planus (OLP) is a common premalignant chronic inflammatory disorder. Optical Coherence Tomography (OCT) provides a real-time, non-invasive, and *in-situ* optical signature using light of varying wavelengths to examine tissue. Aim of the present study was to assess the possible role of OCT as diagnostic tool for atrophic-erosive OLP by examining OCT scans of healthy buccal mucosa, and comparing their ultrastructural features with those of a buccal mucosa affected by atrophic-erosive OLP, using their histopathological counterparts as the gold standard. Through grayscale (enface scan) and an application in which the vascularization of the tissue is visible (dynamic scan), it was possible to distinguish the healthy from the lichenoid pattern from 20 controls (12 M; 8 F; mean age: 41.32 years) and 20 patients with histologically confirmed atrophic-erosive OLP (7 M; 13 F; mean age: 64.27 years). In detail, mean width of stratified squamous epithelium (EP) and lamina propria (LP) were evaluated. Among controls, EP and LP showed a mean width of 300 (±50) and of 600 (±50) μm respectively; among cases, disruption of membrane basement prevented from any measurement. Furthermore, a differential pattern of EP and LP emerged between the two groups: a light-grayish, hypo-reflective, homogeneous area of EP recurring in controls turned into a hyper-reflective, non-homogeneous area among cases. Dynamic scan showed a differential profile of LP vascularization, varying from a hypo-reflective red area with small blood vessels in the control group, to a hypo/hyper-reflective area, completely overrun by a denser, wider blood flow amid OLP cases. Although histopathological examination remains the gold standard for OLP diagnosis, OCT could be a potentially helpful tool for the clinician and the pathologist, since it allows analysis of the vascularization of the sample without adversely affecting histological processing.

1. Introduction

Optical Coherence Tomography (OCT) is a non-invasive imaging technique that employs low-coherence interferometry to generate cross-sectional images of the architecture of a tissue. Typically, OCT relies upon a layout similar to Michelson interferometry, ~~where~~ in which light is divided into two arms: a reference arm and a sample arm. Light in the reference arm is reflected from a mirror to a 2x2 fiber coupler, where it intertwines with the backscattered light coming from the sample under scrutiny, through the sample arm. Such a combination leads to the formation of an interference pattern, which allows calculation of the depth reflectivity pattern of the sample and its conversion into a two-dimensional, high-resolution image. Since 2010, development of Fourier-domain OCT, together with a computer software capable of rapid processing power, enabled real-time scans [1]. OCT has become a reliable diagnostic tool in ophthalmology, with the first report published almost thirty years ago [2], providing relevant data for diagnosis, follow-up and prognosis, especially for neuro-ophthalmology, where it has become one of the most reliable devices in the daily clinical practice [3].

Similarly, OCT showed encouraging application in dermatology, where its potential lies in the diagnosis of non-melanoma skin cancer and basal cell carcinoma, although the high absorption of light caused by melanin and water does lead to a decreased depth of the scan within the skin, in comparison with the eye [1].

Regarding oral disease, potential application of OCT has been described in restorative dentistry for diagnosis of primary and recurrent caries, determination of the accuracy of composite restorations; in endodontics for the identification of additional pulp canals; it may also be of aid in the intraoperative localization of anatomical sites such as inferior alveolar canal and floor of sinus maxillae during implant placement, and helpful in identifying the extent of alveolar bone loss in patients with periodontitis [1, 4-6].

With respect to oral mucosal diseases, few studies have been published, to date, with experimental evidence acquired from narrow sample of patients, ~~with~~ and few comparisons

3

drawn between OCT findings and histological studies, as detailed in a recent systematic review [7].

Oral lichen planus (OLP) is a common chronic inflammatory condition that can affect skin and mucous membranes, including the oral mucosa where it manifests as white, asymptomatic signs, in the form of bilateral, almost symmetrical striae, reticuli, plaques, or red and painful signs, such as atrophy, erosions and ulcers [8-9]. This is a common, and potentially malignant, disorder that usually requires histopathological examination to confirm the diagnosis [10]. In oral medicine, methods that lessen the need for invasive biopsy are ~~thus~~ warranted and constantly explored.

Hence, ~~the~~ aims of the present work were to assess OCT findings in the buccal mucosa of patients with established diagnosis of atrophic-erosive OLP, and to determine the possible differential features between disease-free mucosa and mucosa clinically affected by OLP.

2. Material and Methods

The present trial has been registered with ISRCTN (#17893221), and it was conducted in line with the principles of the Helsinki Declaration of 1975, as revised in 2000 [11]; it was also accepted by the Research Board of the CIR-Dental School, University of Turin.

Two groups of patients have been enrolled, one with appropriate diagnosis of OLP and one with no clinic-histological signs of such disease, with the following selection criteria for "case group" and "control group".

2.1. Case group

2.1.1. First phase: selection by disease

Patients age 18 and older, attending the Oral Medicine Section of the Department of Surgical Sciences, CIR- Dental School (Turin, Italy), either for a first histologic diagnosis of OLP, or as patients already diagnosed with OLP, undergoing clinical follow-up. Specifically, patients with

4

symptomatic atrophic-erosive OLP unexposed to any topical or systemic corticosteroid treatment in the previous 4 weeks were considered eligible for a first selection. Conversely, patients with histologically confirmed diagnosis of other oral premalignant disorder rather than OLP, and patients with previous or concurrent histologic diagnosis of oral squamous cell carcinoma, or other malignancy of head and neck, were excluded.

2.1.2. Second phase: selection by site

The buccal mucosa was considered the most reliable anatomic site to be scanned with OCT, as it was the easiest to be kept stretched by the oral physician for 30 seconds, with minimal to no complaint from the patient. Furthermore, with its plain surface, the buccal mucosa was by far the most appropriate site to maintain a constant contact with the OCT probe, rather than gingiva, ~~where the~~ whose irregularities ~~of~~ from the underlying bone could compromise the quality of the scan, or the tongue, due to its reluctance to remain still for the time necessary to complete the scan.

2.2. Control group

Controls were selected among patients aged 18 and older referred to our Department for excision of traumatic benign lesions of the buccal mucosa (i.e. irritational fibroepithelial polyp, or fibrous hyperplasia). In these cases, a wider diameter of the surrounding healthy buccal mucosa was included in the surgical lozenge, and detached from the original specimen, in order to be evaluated as healthy mucosa by the pathologist. A specific informed consent form was filled and signed by these patients, coupled with the usual informed consent required for biopsy.

2.3. OCT system

A latest variant (OCT oral instrument, version 2.1) of a commercial frequency domain swept source OCT dermatological instrument (SS-OCT, VivoSight® Michelson Diagnostics Ltd,

version 2.0, Orpington, Kent, UK) was deployed. Light source is provided through a Santec HSL-2000 swept laser with the following parameters: wavelength of 1305±15 nm, sweep range of 150 nm, axial and lateral resolutions of <10 μm, depth range of 2 mm, and image width of 6 mm. A probe suitable for oral examination of 124 mm in length, 15 mm in diameter and field of view of 6 mm² was deployed, and kept in contact with the oral site under scrutiny. The probe was enclosed with a thin transparent plastic wrapping around the tip, for an appropriate imaging. Two types of scans can be obtained: "enface" scans – duration: 12 seconds; frames: 120; depth: 6 mm – where the epithelial and sub-epithelial layers can be observed. This device also provides "dynamic" scans – duration: 30 seconds, number of frames: 120, depth: 6 mm – which are a particular subset of "enface" scan, allowing visualization of the underlying vascularization. For the purposes of our study, both enface and dynamic scans were tested and interpreted.

2.4 Histopathologic evaluation

The histopathological evaluation was performed by an optical microscope with 10x magnification. All biopsy specimens were processed by haematoxylin-eosin staining.

The same expert oral pathologist (LC) was asked to describe and measure the average width of the following parameters: keratin layer, epithelial layer, basement membrane, and lamina propria. Further parameters were asked, as follows: hyper/parakeratosis, acanthosis, spongiosis for the epithelial layer, persistence or disappearance of the basement membrane, and characteristics of the inflammatory infiltrate for the lamina propria.

3. Results

3.1. Study groups

Forty consecutive individuals were enrolled. Of these, 20 were cases (13 F; 7 M; mean age 64.27 years) and 20 were controls (8 F; 12 M; mean age 41.32 years).

Table 1 summarizes the main characteristics of the reported sample and the most significant differences of OCT patterns between the two groups.

3.2. Healthy oral mucosa - enface scanning

A recurrent pattern of healthy oral mucosa of the buccal area was detected in the control group (**Fig. 1a**): the cross-sectional OCT scan revealed a light-grayish, hypo-reflective, homogeneous area, with an approximate width of 300 (±50) μm, corresponding to stratified squamous epithelium (EP). With no significant hyper-reflectiveness throughout EP area, and especially in its upper layers, we were able to infer the absence of a keratinized layer, as expected in the epithelium of a lining mucosa.

Beneath EP, a whitish, hyper-reflective, non-homogenous area, with an approximate width of 600 (±50) μm was detected, corresponding to the underlying lamina propria (LP).

The difference in reflectiveness and homogeneity between EP and LP might be caused by the overall homogeneity of EP, leading to a lower backscattering signal, whereas LP, a dense fibrous connective tissue with embedded blood vessels and nerves, might display a more non-homogeneous pattern, leading to a higher backscattering signal in the OCT cross-sections.

Beneath LP, where the deepest layers of connective/muscular tissue are histologically detectable, a homogenous dark area appeared, suggestive of the ultimate boundary of OCT scan, preventing further evaluation. Figure 1b shows the histologic counterparts of the aforementioned OCT features.

3.3. Healthy oral mucosa - dynamic scanning

Cross-sectional dynamic scan ~~is~~ was able to reveal the vascularization within LP, where the dense fibrous connective tissue with embedded small caliber blood vessels emerged as a hypo-reflective red area with a mottled pattern, intertwined through serpiginous red "spikes" with the

overlying epithelium. In the homogeneous dark area beneath LP, in which the enface scan could not allow any further analysis, this red mottled pattern appeared, as well (**Fig. 2**).

3.4. OLP mucosa - enface scanning

The main and most recurring change of OLP mucosa at enface scan could be found within LP (**Fig. 3**), where the distinct hyper-reflectiveness area is almost completely lost, leading to further difficulties in recognizing the transition between the overlying epithelium and the underlying connective tissue. On the other hand, the epithelium itself can present less width, and an unexpected higher propensity for hyper-reflectiveness, indicative of either hyperkeratosis or hyperparakeratosis.

3.5. OLP mucosa - dynamic scanning

The most recurring alteration of OLP mucosa at the dynamic scan is the scattered red dots emerging throughout the grey, non-homogenous, hyper-reflectiveness of EP. Such condition might be attributed to the concurrent intra and inter-cellular oedema, as expected in cases of acanthosis and spongiosis, with both being typical ultrastructural manifestations of OLP. On the other hand, LP revealeds, together with the loss of integrity and hyper/hypo-reflectiveness of the lamina propria, an increased, denser red pattern of vascularization, indicative of a higher blood inflow within a chronically-inflamed mucosa (**Fig. 4a**). Figure 4b shows the histologic counterparts of the aforementioned OCT features.

4. Discussion

OCT technology has evolved rapidly and substantially since the first reports of its value for assessing the skin [12]. As a fast, non-invasive tool being able to provide high-resolution imaging of vascularization, it is routinely deployed in ophthalmology for a wide range of retinal disorders, including uveitis, maculopathy and diabetic neuropathy [13,14]. In the past few

8

years, advancement of OCT technology induced a widespread application as a promising tool in dermatology, where OCT was tested on neoplastic disorders, enabling the differentiation of non-melanoma skin cancers from benign lesions and normal skin, in vivo differentiation of histological subtypes of basal cell carcinoma, and grading of actinic keratosis [15-17].

OCT showed promising results on an extensive spectrum of inflammatory disorders of the skin, especially those defined by changes within the epithelium and dermo-epidermal junction, such as pemphigus, bullous pemphigoid and lichen planus [1], which can each also arise within the oral cavity.

The aim of this preliminary study was to evaluate the differential epithelial and sub-epithelial pattern of healthy and OLP-affected buccal mucosa, with a newly-designed probe which, to our knowledge, has only been tested for ex-vivo examination of nonmelanoma skin cancer [18].

The present work revealed distinct ultrastructural differences between healthy controls and patients affected by atrophic-erosive OLP, with a very close agreement between OCT and histopathology scores, in terms of reduction of epithelial width and display of hyperparakeratosis, loss of integrity of basement membrane, heavy inflammatory infiltration and increased vascularization within the lamina propria.

Thus, the main strength of the present work relies on the novelty of the approach. To the best of our knowledge, few studies have explored the OCT characteristics of cutaneous and ocular Lichen Planus [19,20]. Furthermore, no previous article explored the potential of the dynamic scans of OCT in revealing the ultrastructural modifications of the epithelium and the underlying connective tissue. Conversely, the goal of OCT in the supervision of potentially malignant lesions and oral cancer has been explored in oral medicine, and described in some articles, partially in vivo and especially ex vivo [21,22]. However, the difference between healthy tissue and tissue undergoing transformation was focused on the differences in terms of increased thickness of the epithelial layer and of the keratinized epithelial surface layer, a higher hyper-

reflectivity within the epithelial layers, loss of integrity of the basement membrane and of the surrounding structures [23-25].

In the present work, it would be appropriate to justify the reduction of the thickness of the epithelial layer detected amid OLP cases as a consequence of the strict inclusion criteria, with patients affected by atrophic-erosive OLP being the only eligible for the present study. By definition, such form of OLP is expected to display a clinical and morphological reduction of epithelial width and integrity.

The present results appear promising, in suggesting that OCT can be an additional mean of investigating OLP, being a non-invasive tool with no biologic costs, able to provide a complete scan in just thirty seconds. Several studies have reported an overall high sensitivity and specificity for OCT to intercept oral potentially malignant disorders and oral cancer. A very recent critical review reported an overall sensitivity of 80-90%, and a specificity of 85-98% [26]. However, the use of OCT may have some limitations. The presently employed oral probe may not be appropriate for some areas of the mouth often affected by OLP – in particular areas such as tongue and gingiva. Whenever tested, the flat surface of the probe deployed in this study, although long enough to potentially reach the furthest sites, was often unsuitable for convex, irregular surfaces of palate and gingiva, as well as on the tongue, due to the difficulty of the patient and/or the clinician to hold it perfectly still during scanning. Moreover, the necessity for a close contact with the mucosa might lead to artefacts within the scan, if an unexperienced clinician was to apply an excessive pressure on the district under scrutiny, usually detectable as unreadable "red flares" at the dynamic scan.

A further limitation is the necessity for appropriate training in OCT usage and interpretation of the scans. The latter is an issue that must be addressed, especially in oral medicine, considering the scattered evidences available, with scans achievable from different OCT devices, pursued on different clinical entities, and no universal consensus available on the potential role of OCT in this field.

10

Further research should focus on the design of an oral probe capable of enough versatility to be applied in every mucosal district, ideally with a no-contact approach. Moreover, the machine should be equipped with an appropriate software capable of magnifying more appropriately epithelial alterations, especially regarding the lower third of epithelium, and of a 3-D reconstruction of the sample. Studies of larger study groups will be then necessary to determine the sensitivity and specificity of such preliminary OCT findings in patients with atrophic-erosive OLP. To date, histology remains the gold standard for diagnosis of OLP; however, OCT might play a role in the follow-up of this chronic inflammatory disease, to assess the efficacy of a specific protocol, or to draw a comparison between treatments in patients unresponsive to topical corticosteroids, which represent the first line of treatment.

Declaration of Competing Interest

The authors state no conflict of interest.

Author Contributions

Conceptualization: AC, RB, PGA, SRP, AG, CH; Formal Analysis: MC, AG, AC, LC; Funding Acquisition: SC, SRP, CH; Investigation: MC, AG, AC, LG; Methodology: PGA; AC; AG; MC; RB; Project administration: PGA, RB, SRP, SC; Software: AG, MC, AC; Supervision: SC, RB, PGA, CH, SRP; Validation: AG, PGA, MC, SRP; Visualization: AG, MC, PGA, AC, SRP; Writing - Original Draft Preparation: AG, MC, PGA, SRP; Writing - Review and Editing: RB, SRP, PGA, MC, AG.

References

[1] Olsen J, Holmes J, Jemec GB. Advances in optical coherence tomography in dermatology-a review. J Biomed Opt. 23(2018) 1-10, doi: 10.1117/1.JBO.23.4.040901.

 [2] Huang D, Swanson EA, Lin CP, Schuman JS, Stinson WG, Chang W, Hee MR, Flotte T, Gregory K, Puliafito CA. Optical coherence tomography. Science. 254 (1991) 1178-1181, doi: 10.1126/science.1957169

[3] Rebolleda G, Diez-Alvarez L, Casado A, Sánchez-Sánchez C, de Dompablo E, González-López JJ, Muñoz-Negrete FJ. OCT: New perspectives in neuro-ophthalmology. Saudi J Ophthalmol. 29 (2015) 9-25, doi: 10.1016/j.sjopt.2014.09.016.

[4] Luong MN, Shimada Y, Araki K, Yoshiyama M, Tagami J, Sadr A. Diagnosis of Occlusal Caries with Dynamic Slicing of 3D Optical Coherence Tomography Images. Sensors (Basel). 20 (2020). pii: E1659, doi: 10.3390/s20061659.

[5] Tsubokawa M, Aoki A, Kakizaki S, Taniguchi Y, Ejiri K, Mizutani K, Koshy G, Akizuki T, Oda S, Sumi Y, Izumi Y. In vitro and clinical evaluation of optical coherence tomography for the detection of subgingival calculus and root cementum. J Oral Sci. 60 (2018) 418-427, doi: 10.2334/josnusd.17-0289.

[6] Sanda M, Shiota M, Imakita C, Sakuyama A, Kasugai S, Sumi Y. The effectiveness of optical coherence tomography for evaluating peri-implant tissue: A pilot study. Imaging Sci Dent. 46 (2016) 173-178, doi: 10.5624/isd.2016.46.3.173.

[7] Gentile E, Maio C, Romano A, Laino L, Lucchese A. The potential role of in vivo optical coherence tomography for evaluating oral soft tissue: A systematic review. J Oral Pathol Med. 46 (2017) 864-876, doi: 10.1111/jop.12589.

[8] Warnakulasuriya S. Clinical features and presentation of oral potentially malignant disorders. Oral Surg Oral Med Oral Pathol Oral Radiol. 125 (2018) 582-590, doi: 10.1016/j.oooo.2018.03.011.

[9] Carbone M, Arduino PG, Carrozzo M, Gandolfo S, Argiolas MR, Bertolusso G, Conrotto D, Pentenero M, Broccoletti R. Course of oral lichen planus: a retrospective study of 808 northern Italian patients. Oral Dis. 15 (2009) 235–243, doi: 10.1111/j.1601-0825.2009.01516.x.

[10] Gandolfo S, Richiardi L, Carrozzo M, Broccoletti R, Carbone M, Pagano M, Vestita C, Rosso S, Merletti F. Risk of oral squamous cell carcinoma in 402 patients with oral lichen planus: a follow-up study in an Italian population. Oral Oncol. 40 (2004) 77–83, doi: 10.1016/s1368-8375(03)00139-8

[11] Wma.net. 2020. WMA - The World Medical Association-Declaration Of Helsinki 2000. [online] Available at: <https://www.wma.net/what-we-do/medical-ethics/declaration-of-helsinki/doh-oct2000/> [Accessed 4 July 2020].

[12] Welzel J, Lankenau E, Birngruber R, Engelhardt R. Optical coherence tomography of the human skin. J Am Acad Dermatol. 37 (1997) 958-963, doi: 10.1016/s0190-9622(97)70072-0

[13] Kashani AH, Chen CL, Gahm JK, Zheng F, Richter GM, Rosenfeld PJ, Shi Y, Wang RK. Optical coherence tomography angiography: A comprehensive review of current methods and clinical applications. Prog Retin Eye Res. 60 (2017) 66-100, doi: 10.1016/j.preteyeres.2017.07.002.

[14] Wang JC, Miller JB. Optical Coherence Tomography Angiography: Review of Current Technical Aspects and Applications in Chorioretinal Disease. Semin Ophthalmol. 34 (2019) 211-217, doi: 10.1080/08820538.2019.1620797.

[15] Boone MA, Suppa M, Pellacani G, Marneffe A, Miyamoto M, Alarcon I, Ruini C, Hofmann-Wellenhof R, Malvehy J, Jemec GB, Del Marmol V. High-definition optical coherence tomography algorithm for discrimination of basal cell carcinoma from clinical BCC imitators and differentiation between common subtypes. J Eur Acad Dermatol Venereol. 29 (2015) 1771-1780, doi: 10.1111/jdv.13003.

[16] Marneffe A, Suppa M, Miyamoto M, Del Marmol V, Boone M. Validation of a diagnostic algorithm for the discrimination of actinic keratosis from normal skin and squamous cell carcinoma by means of high-definition optical coherence tomography. Exp Dermatol. 25 (2016) 684-687, doi: 10.1111/exd.13036

[17] Mogensen M, Joergensen TM, Nürnberg BM, Morsy HA, Thomsen JB, Thrane L, Jemec GB.. Assessment of optical coherence tomography imaging in the diagnosis of non-melanoma skin cancer and benign lesions versus normal skin: observer-blinded evaluation by dermatologists and pathologists. Dermatol Surg. 35 (2009) 965-972, doi: 10.1111/j.1524-4725.2009.01164.x.

[18] Rashed D, Shah D, Freeman A, Cook RJ, Hopper C, Perrett CM. Rapid ex vivo examination of Mohs specimens using optical coherence tomography. Photodiagnosis Photodyn Ther. 19 (2017) 243-248, doi: 10.1016/j.pdpdt.2017.06.006.

[19] Ianoși SL, Forsea AM, Lupu M, Ilie MA, Zurac, Boda D, Ianosi G, Neagoe D, Tutunaru C, Popa CM, Caruntu C. Role of modern imaging techniques for the in vivo diagnosis of lichen planus. Exp Ther Med. 17 (2019) 1052-1060, doi: 10.3892/etm.2018.6974.

[20] Ozlu E, Teberik K. Evaluation of ocular findings in patients with lichen planus. Postepy Dermatol Alergol. 36 (2019) 267-271, doi: 10.5114/ada.2018.74464.

[21] Jung W, Zhang J, Chung J, Wilder-Smith P, Brenner M, Nelson JS, Chen Z. Advances in oral detection using optical coherence tomography. IEEE J Scl Top Quantum Electron. 11 (2005) 811-817.

[22] Tsai MT, Lee HC, Lee CK, Yu CH, Chen HM, Chiang CP, Chang CC, Wang YM, Yang CC. Effective indicators for diagnosis of oral cancer using optical coherence tomography. Opt Express. 16 (2008) 15847-15862, doi: 10.1364/oe.16.015847

[23] DeCoro M, Wilder-Smith P. Potential of optical coherence tomography for early diagnosis of oral malignancies. Expert Rev Anticancer Ther. 10 (2010) 321-329, doi: 10.1586/era.09.191.

[24] Pande P, Shrestha S, Park J, Serafino MJ, Gimenez-Conti I, Brandon J, Cheng YS, Applegate BE, Jo JA. Automated classification of optical coherence tomography images for the diagnosis of oral malignancy in the hamster cheek pouch. J Biomed Opt. 19 (2014) 086022, doi: 10.1117/1.JBO.19.8.086022.

[25] Jerjes W, Hamdoon Z, Yousif AA, Al-Rawi NH, Hopper C. Epithelial tissue thickness improves optical coherence tomography's ability in detecting oral cancer. Photodiagnosis Photodyn Ther. 28 (2019) 69-74, doi: 10.1016/j.pdpdt.2019.08.029.

[26] Ilhan B, Lin K, Guneri P, Wilder-Smith P. Improving Oral Cancer Outcomes with Imaging and Artificial Intelligence. J Dent Res. 99 (2020) 241-248, doi: 10.1177/0022034520902128.

Table 1. Main characteristics of the two samples and related OCT findings.

Group	Size of sample	M/F ratio	Mean age	Mean width of EP (enface scan)	Mean width of LP (enface scan)	Visual characteristics of EP (enface scan)	Visual characteristics of LP (enface scan)	Visual characteristics of EP (dynamic scan)	Visual characteristics of LP (dynamic scan)
Controls	20	12/8	41.32 yo	300 (±50) μm	600 (±50) μm	Light-grayish, hypo-reflective, homogeneous area of precise and recurring width	Whitish, hyper-reflective, non-homogeneous area of precise and recurring width	Mostly unchanged when compared to enface scan	Hypo-reflective red area with mottled pattern, intertwined through serpiginous red "spikes" with overlying EP (physiological distribution of small and medium-sized blood vessels)
Cases	20	7/13	64.27 yo	NA	NA	Hyper-reflective, non-homogeneous area, of unquantifiable width	Hypo/hyper-reflective, non-homogeneous area, of unquantifiable width	Hyper-reflective, non-homogeneous area with scattered red dots in the first 100 (±15) μm (paracheratosis and granulocyte exocytosis) and in the underlying 200 (±15) μm (lymphocyte and granulocyte exocytosis)	Hypo/hyper-reflective area, completely covered by denser, wider and higher red "spikes" (pathologic blood inflow caused by OLP-related chronic inflammation)

EP: squamous stratified epithelium; **LP**: lamina propria; NA: not available; **yo**: years-old

FIGURE 1a. Pattern of healthy buccal mucosa at OCT enface scan. **A**: stratified squamous epithelium (EP) as grayish, hypo-reflective, homogeneous area; **B**: underlying lamina propria (LP) as hyper-reflective, non-homogenous area; **C**: deepest layers of connective/muscular tissue as unreadable homogenous dark area; **1b.** Histological pattern of healthy buccal mucosa with 10x optical microscope magnification - hematoxylin-eosin staining. **A**: stratified squamous epithelium **B**: lamina propria **C**: connective tissue.
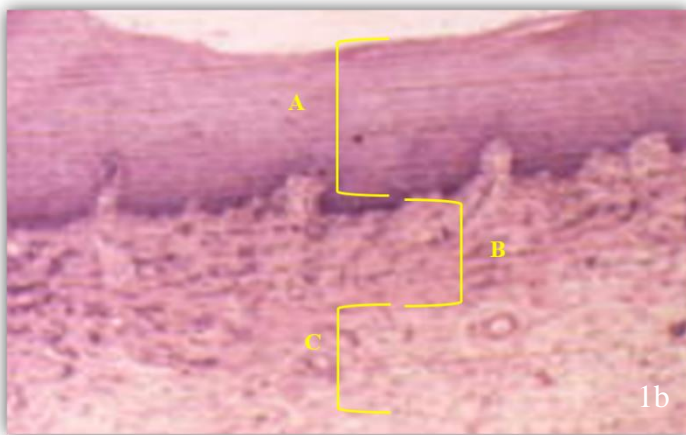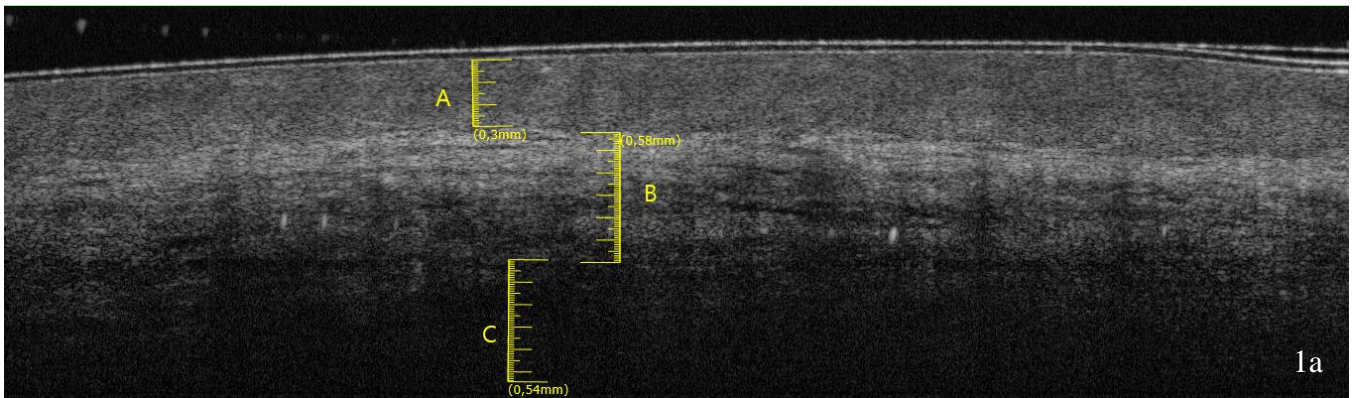
FIGURE 2. Pattern of healthy buccal mucosa at OCT dynamic scan. **A:** stratified squamous epithelium (EP) displaying overlapping characteristics as in Fig.1a; **B:** vascularization within lamina propria (LP), as a hypo-reflective red area. Notice the mottled pattern, and the serpiginous red "spikes" at the interface with overlying EP. **C:** red mottled pattern emerging partially within the homogeneous dark area beneath LP.
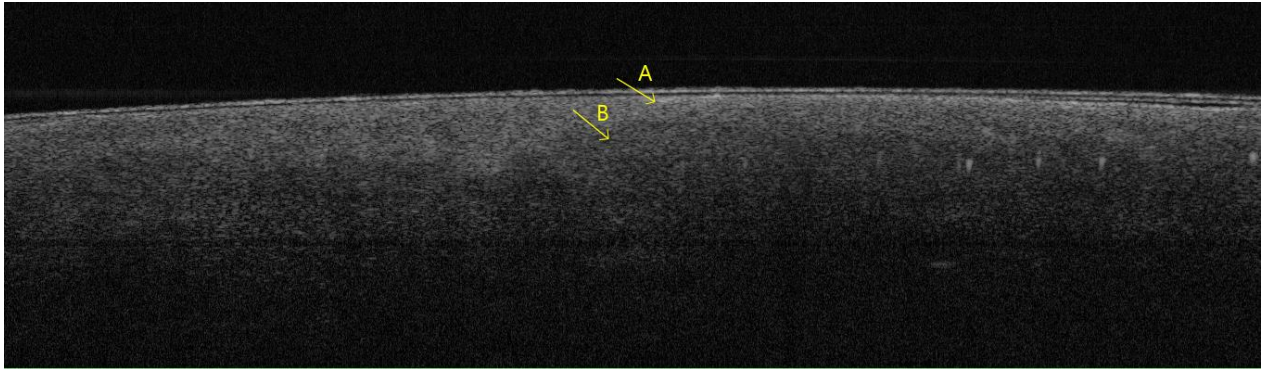
FIGURE 3. Pattern of buccal mucosa affected by OLP at OCT enface scan. **A:** stratified squamous epithelium (EP) with less width, and higher hyper-reflectiveness, indicative of either hyperkeratosis or hyperparakeratosis; **B:** lamina propria (LP) with almost complete lack of distinct hyper-reflectiveness and of a clear transition between EP and LP.
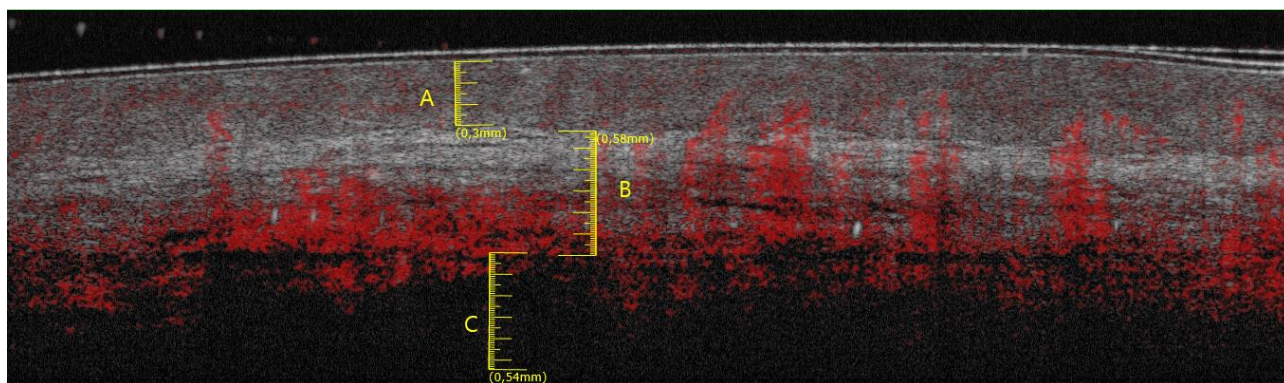
FIGURE 4a. Pattern of buccal mucosa affected by OLP at OCT dynamic scan. **A**: scattered red dots in the first 100 (±15) μm of stratified squamous epithelium (EP), corresponding to the pathologic finding of parakeratosis and granulocyte exocytosis. **B**: scattered red dots in the underlying 200 (±15) μm of stratified squamous epithelium (EP), corresponding to the pathologic finding of lymphocyte and granulocyte exocytosis; **C**: enriched inflammatory infiltrate within the 500 μm of lamina propria (LP). Notice the increased, denser red pattern of vascularization when compared to Fig.2, area "B", indicative of a higher blood inflow typical of a chronically-inflamed mucosa **D**: remaining layers of the deepest fibrous stroma, as a dark, unreadable area. **TW**: total width of the sample (1 mm). **Fig 4b**. Histologic counterpart of pattern of buccal mucosa affected by OLP - 10x optical microscope magnification - hematoxylin-eosin staining. **A**: findings of parakeratosis and granulocyte exocytosis 100 (±15)μm of EP . **B**: pathologic finding of lymphocyte and granulocyte exocytosis 200 (±15) μm of EP; **C**: enriched inflammatory infiltrate within the 500 μm of lamina propria (LP); **D**: remaining layers of the deepest fibrous stroma with large caliber vessels. **TW**: total width of the sample (1 mm).